J. Med. Biol. Eng. (2015) 35:236–241
DOI 10.1007/s40846-015-0019-6

ORIGINAL ARTICLE

Primary Stability of Absorbable Screw Fixation for Intra-articular Calcaneal Fractures: A Finite Element Analysis

Ming Ni[1,2] · Xiao-Hong Weng[4,5] · Jiong Mei[1] · Wen-Xin Niu[3]

Received: 12 July 2013 / Accepted: 26 March 2014 / Published online: 26 March 2015

Abstract Absorbable implants have been widely used in bone osteosynthesis, but biomechanics of its application to calcaneal fracture fixation remains unclear. This study investigates the primary stability of absorbable screws used to fix calcaneal fractures with the finite element method. A Sanders type III calcaneal fracture was modeled according to X-ray and computed tomography images of a representative patient. Fixation with four crossing absorbable screws was simulated using a finite element software package according to clinical operation. The stance phase of gait was simulated to calculate stress and displacement distributions of the calcaneus and screws. The stress concentration of screws was located at the connections between screws and fracture surfaces. For the two transverse screws, the peak von Mises stress of the inferior screw was almost twice that of the superior one. For the two longitudinal screws, the medial screw had a 64 % larger von Mises stress than that of the lateral one. The peak displacement of the calcaneus was located on the medial fragment. No notable relative displacement was seen between different fragments. The displacements of the two transverse screws were similar, and larger than those of the longitudinal screws. The displacement of the medial longitudinal screw was slightly greater than that of the lateral one. Based on the computational stress distribution, a screw with a large diameter should be recommended to fix the anterior part of the posterior facet and the medial tuberosity of the calcaneus. Fixation with crossing absorbable screws is safe and should be recommended for Sanders type III intra-articular calcaneal fractures with good bone quality. Early ambulation and rehabilitational activities should be encouraged after operation.

Keywords Calcaneal fractures · Finite element method · Absorbable implant · Screw fixation · Biomechanics

1 Introduction

The incidence of calcaneal fractures comprises around 2 % of all fractures presenting to emergency departments and the proportion of intra-articular calcaneal fractures with involvement of the posterior subtalar joint is approximately 75 % [1]. Open reduction and plating fixation with plates and screws is widely used for intra-articular calcaneal fractures. However, the high incidence of wound infections has prejudiced surgeons against operative treatment [2, 3]. In order to minimize wound complications while providing relatively rigid fixation for calcaneal fractures, percutaneus screw fixation is adopted by many surgeons due to its simple operation, rigid fixation, and few complications [4, 5].

Absorbable poly-L-lactide acid (PLLA), an orthopedic implant material, has a mechanical strength similar to that

✉ Wen-Xin Niu
niu@tongji.edu.cn

1 Tongji Hospital, Tongji University School of Medicine, Shanghai 201200, China

2 Department of Orthopedics, Pudong New Area People's Hospital, Shanghai 200065, China

3 Yang Zhi Rehabilitation Hospital, Tongji University School of Medicine, Shanghai 201619, China

4 Key Laboratory for Biomechanics and Mechanobiology of Ministry of Education, School of Biological Science and Medical Engineering, Beihang University, Beijing 100191, China

5 Chinese Society of Biomedical Engineering, Beijing 100005, China

of cortical bone [6, 7]. In the past 40 years, absorbable implants have been widely used in many types of bone osteosynthesis, including calcaneal fractures [8–10]. The application of absorbable implants can avoid the subsequent removal of implants. Bone fractures fixed with absorbable implants can be more clearly observed in X-rays due to the lack of interference from metallic components. Min et al. [10] introduced a technique that uses absorbable pin fixation to maintain an anatomic reduction of the posterior facet in displaced intra-articular calcaneal fractures. They found this technique to be advantageous for multiple reasons, such as simplifying manipulation and repositioning during final fixation, obviating the use of K-wires during provisional fixation, minimizing the problems associated with "screw traffic", and minimizing the morbidity and failure rates associated with bioabsorbable implants [10]. However, the biomechanical stability of calcaneal fractures fixed with absorbable screws has not been studied. Surgeons have little knowledge to instruct patients about rehabilitation training after operation.

Finite element analysis (FEA) is a powerful and reliable biomechanical tool. It can be used to calculate the stress and displacement distribution of a model in each detail [11–14]. For example, Lee and Lee [12] constructed a finite element (FE) model that included the talus and calcaneus to assess the optimal configuration of double-screw fixation for subtalar arthrodesis. However, there has been no FEA report concerning the primary stability of calcaneal fractures fixed with absorbable screws.

Therefore, the aim of this study was to construct an FE model of calcaneal fractures fixed with bioabsorbable screws and to evaluate the primary stability of such fixation during the stance phase of gait. Based on previous experiences in clinics and mechanics, it was hypothesized that the stress concentration would occur at the connection between the screws and bone tissue and that the peak values would not be larger than the strengths of both screws and bone.

2 Materials and Methods

Between July 2008 and December 2012, nine patients with intra-articular calcaneal fractures were treated with percutaneous reduction and absorbable screw fixation (Grand Fix, Gunze Co., Ltd., Tokyo, Japan) in the Department of Orthopedics, Pudong New Area People's Hospital, China. All patients underwent X-ray and computed tomography (CT) scanning examinations. According to the Sanders scale based on the CT images, three of the fractures were classified as type II and the remaining six were classified as type III. The common characteristics of the nine fractures according to X-ray and CT images were a V-shaped compression of the calcaneal body and two or three partial fractures of the poster subtalar articular without obvious bone defects (Fig. 1). PLLA absorbable screws were used. All fractures were reduced postoperatively and healed and patients were able to resume their jobs.

The right foot of a normal Chinese male (age: 30 years; body weight: 70 kg; height: 173 cm) was CT scanned in the neutral position by a CT scanner (Brilliance 64 CT, Philips Electronics, The Netherlands). The slice thickness of CT scanning was 0.630 mm. 339 slices were obtained. The CT images were imported into image processing software MIMICS 15.0 (Materialise, Leuven, Belgium), in which the bone contour was obtained. Then, a solid model of the calcaneus was constructed in Unigraphics NX 8.5 (Siemens, Germany). A Sanders type III calcaneal fracture was modeled according to the common characteristics of the nine fractures. As shown in Fig. 2, fixation with four absorbable screws was simulated according to clinical operation. The diameter and length were 3.5 and 45 mm for the transverse screws and 7.0 and 80 mm for the

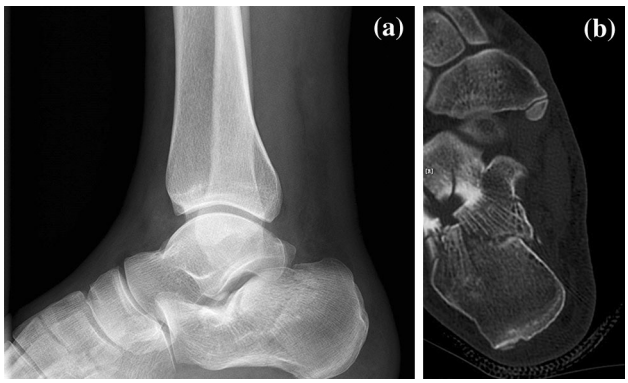

Fig. 1 **a** X-ray and **b** CT images of intra-articular calcaneal fractures

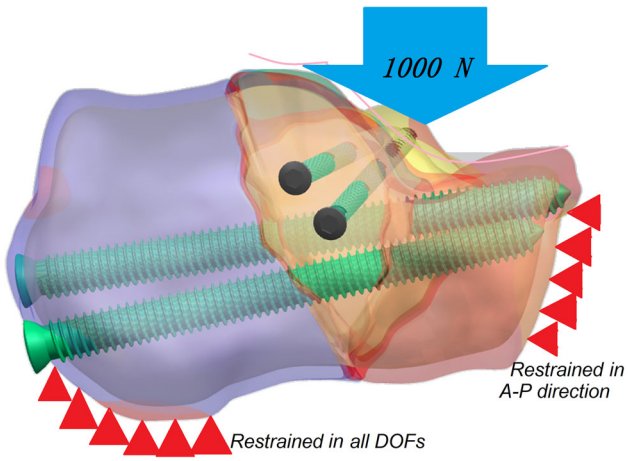

Fig. 2 Three-dimensional reconstruction model and boundary and loading conditions (*DOF* degree of freedom, *A–P* anterior–posterior)

longitudinal screws, respectively. The pitch of all screws was 1.25 mm.

The model of the calcaneal fractures fixed by absorbable screws was imported into and assembled in the FE analysis package ANSYS 13.0 (Swanson Analysis, Houston, PA). The contact between screws and the calcaneus was defined as bonded in this model. Niu and Ding [17] previously compared three methods used in FE modeling of the calcaneus. They conducted a convergence test and found that 137 k degrees of freedom ensured steady computations of the displacement and von Mises stress. In the present study, the model had several contact surfaces between different fragments and between bone and implants. A fine mesh (320,341 nodes and 210,237 quadratic tetrahedral elements) was constructed to simulate the surgery. A convergence test showed that further mesh refinement resulted in computations differing by less than 2 %. The cortical and cancellous bones and the implants were idealized as homogenous, isotropic, and linearly elastic. The thick of cortical bone was set as 0.5 mm.

The mechanical properties of the bones and absorbable screws were selected from previous published reports [15–17]. They are listed in Table 1. Young's modulus is a fundamental measure of the stiffness of an elastic material, and a necessary input parameter for FE simulation. Although the material property of calcaneal bone is anisotropic and nonlinear, it can be simplified as isotropic linear elastic in FEA while maintaining good accuracy [11, 17]. The coefficient of friction between fragments was set as 0.2.

The loading and boundary conditions are detailed in Fig. 2. Based on previous experiments, the force on the Achilles tendon was 780 N at 70 % of the stance phase [18] and the ground reaction force on the heel was about 220 N during unipedal standing [19, 20]. Therefore, to maintain equilibrium in the vertical direction, a loading of 1000 N was applied on the subtalar articular surfaces of the calcaneus, while the posteroinferior calcaneal tuberosity was limited to 6 degrees of freedom. To simplify the loading and boundary conditions, the calcaneocuboid and talocalcaneonavicular joints were also restrained in the anterior-posterior direction. The peak von Mises stress was calculated for each part of this model. The von Mises stress is based on the von Mises yield criterion, which assumes that the material yielding begins when the second deviatoric stress invariant reaches a critical value. Its peak value is often used in biomechanics to evaluate and predict tissue injuries [11, 13, 17].

Table 1 Mechanical properties of cortical and cancellous bones and absorbable screws [15–17]

Material	Young's modulus (MPa)	Poisson's ratio
Cortical bone	10,000	0.3
Cancellous bone	1450	0.2
Absorbable implants	1400	0.2

3 Results

The von Mises stress peaks of all screws are listed in Table 2, and the stress distributions are shown in Fig. 3. The stress concentration of screws was located at the connections between screws and fracture surfaces. For the two transverse screws, the peak von Mises stress of the inferior screw was 133 MPa, almost twice that of the superior one (68 MPa). For the two longitudinal screws, the medial screw (117 MPa) had a 64 % larger von Mises stress than that of the lateral one (71 MPa).

The peak displacements of the calcaneus and all screws are listed in Table 3. The peak displacement of the calcaneus was located on the medial fragment. No notable relative displacement was seen between different fragments. As shown in Fig. 4, the displacements of the two transverse screws were similar, and larger than those of the longitudinal screws. The displacement of the medial longitudinal screw was slightly greater than that of the lateral one.

4 Discussion

In foot and ankle surgery, absorbable implants are used in trauma and bone operations [10, 21, 22]. The modulus of elasticity of absorbable implants is close to that of cortical bone, which makes them safe for internal ankle or calcaneal fractures. Because absorbable implants are weaker than metallic ones, patients with calcaneal fractures fixed by absorbable implants have their rehabilitation restricted early on to avoid implant breakage and bone refractures [22].

There have been several biomechanical studies on the stability of calcaneal fractures fixed with various implants [23–26]. Wang et al. [23] compared the strength of two

Table 2 Von Mises stress peaks of all screws (MPa)

Screw	Stress
Inferior transverse	133
Superior transverse	68
Medial longitudinal	117
Lateral longitudinal	71

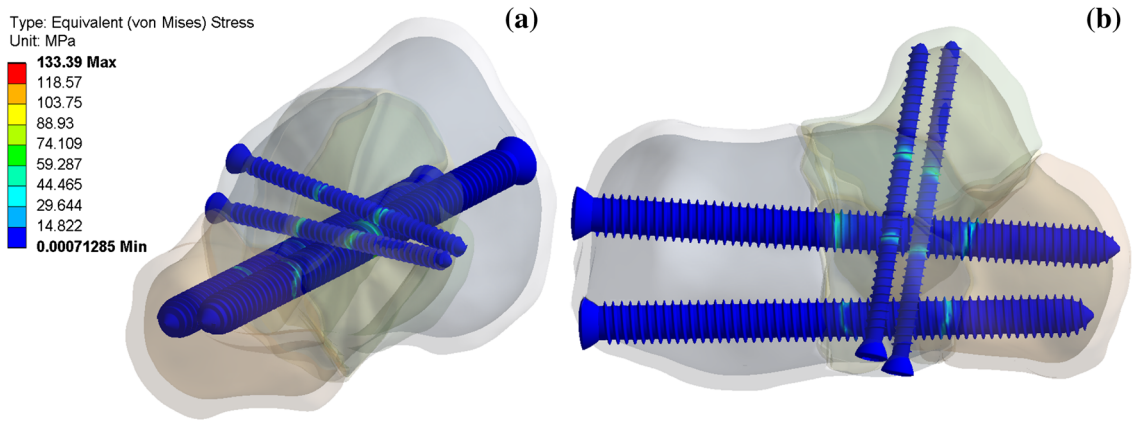

Fig. 3 Distribution of von Mises stress of all screws. **a** Anterior-medial view and **b** superior screw

Table 3 Peak displacements of calcaneus and screws (mm)

Location	Displacement
Calcaneus	0.40
Inferior transverse	0.36
Superior transverse	0.38
Medial longitudinal	0.17
Lateral longitudinal	0.13

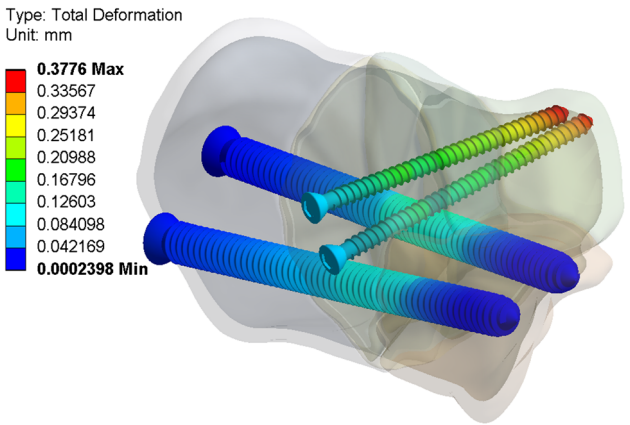

Fig. 4 Distribution of resultant displacement of all screws

types of fixation method for calcaneal fractures. Redfen et al. [24] compared the mechanical integrity of locking plate and traditional non-locking plate fixation for calcaneal fractures. Nelson et al. [25] evaluated the stability of a new headless screw technique for calcaneal fractures. Richter et al. [26] compared the stability of a calcaneal plate with polyaxially locked screws with 3 plates fixed with uniaxially locked screws. All these studies used cadaveric or physical models to reconstruct the fractures and fixation. However, few parameters can be measured through mechanical experiments and experimental cost is very high. Many important parameters, such as displacement, stress, and strain at any location, are difficult to measure using current techniques.

In this study, a three-dimensional FE model was used to analyze the primary stability of absorbable screw fixation for intra-articular calcaneal fractures. The stress and displacement distributions of the screws and calcaneus fragments during the stance phase of walking gait were obtained. The FEA computation showed that the stress concentration of screws was located at the connections between screws and fracture surfaces. The screws were thus the main support structures for the bodyweight loading.

In FE calculation, the stress at the connections of different materials has a larger computational error than that for homogeneous materials. Although the computational error often results in higher stress, comparisons of stress between screws in a given model can produce useful results. The stress distribution of screws in each group was similar, but the maximum stress was different. In the transverse group, the maximum stress of the inferior screw was much higher than that of the superior one. This result is consistent with those from biomechanical experiments [23, 27]. Wang et al. [27] showed that the peak stress sustained in the subtalar joint is concentrated at the anterior part of the posterior facet, which was the position of the inferior screw. The medial longitudinal screw had a larger von Mises stress than that of the lateral one. A screw with a large diameter should be recommended to fix the anterior part of the posterior facet and the medial tuberosity of the calcaneus.

The maximum von Mises stress of screws was 133 MPa. Although this value might be overestimated due to computational error, it is less than the bending strength (176–215 MPa) [7] and shear strength (143.6 MPa) of PLLA [6]. The results show that absorbable screws are safe

for calcaneal fracture fixation. Patients with calcaneal fractures fixed with absorbable screws should be encouraged to begin rehabilitation soon after operation. However, high-impact activities such as running should be avoided as the loading on the calcaneus would be several times the level while standing [28].

The displacements of the medial parts of both the calcaneus and screws were greater than those of the lateral parts. The pressure distribution of the subtalar joint was inhomogeneous, and the pressure in the medial parts was higher than that in the lateral parts [29]. The pressure distribution had a great influence on the displacements of the calcaneus and screws. The higher pressure and displacements of the medial calcaneus showed that the medial part of the calcaneus should be restored as much as possible in the operation. A bone graft should be performed for calcaneal fractures with obvious bone defects.

There were several limitations in this study. Firstly, only the Sanders type III intra-articular calcaneal fracture was simulated in the FEA. More biomechanical and clinical research should be carried out on other types of fracture in the future. Secondly, the material properties of the calcaneal bone were determined according to the average of a population. For special patients, such as those with osteoporosis, fixation with absorbable screws will have higher risks because of its lower strength compared to that of traditional metallic implants. Finally, soft tissues and other neighboring structures were not included in the model because of the difficulty in modeling and analysis. Nevertheless, the simplified model used here provided useful results. These limitations will be considered in future studies.

5 Conclusion

An FE model was used to analyze the primary stabilization of absorbable screw fixation for intra-articular calcaneal fractures. Based on the computational stress distribution, a screw with a large diameter should be recommended to fix the anterior part of the posterior facet and the medial tuberosity of the calcaneus. Fixation with crossing absorbable screws is safe for patients with good bone quality and should be recommended for Sanders type III intra-articular calcaneal fractures. Early ambulation and rehabilitational activities are encouraged after operation.

Acknowledgments This study was supported by the Youth Science & Technology project of Shanghai Health Burean (20134Y207), and the National Science Foundation of China (NSFC 11302154).

References

1. Schepers, T., van Lieshout, E. M., van Ginhoven, T. M., Heetveld, M. J., & Patka, P. (2008). Current concepts in the treatment of intra-articular calcaneal fractures: results of a nationwide survey. *International Orthopaedics, 32*, 711–715.
2. Schepers, T., Den Hartog, D., Vogels, L. M., & Van Lieshout, E. M. (2013). Extended lateral approach for intra-articular calcaneal fractures: an inverse relationship between surgeon experience and wound complications. *Journal of Foot and Ankle Surgery, 52*, 167–171.
3. Benirschke, S. K., & Kramer, P. A. (2004). Wound healing complications in closed and open calcaneal fractures. *Journal of Orthopaedic Trauma, 18*, 1–6.
4. Fu, T. H., Liu, H. C., Su, Y. S., & Wang, C. J. (2013). Treatment of displaced intra-articular calcaneal with combined transarticular external fixation and minimal internal fixation. *Foot and Ankle International, 34*, 91–98.
5. Kesemenli, C. C., Memisoglu, K., & Atmaca, H. (2013). A minimally invasive technique for the reduction of calcaneal fractures using the Endobutton®. *Journal of Foot and Ankle Surgery, 52*, 215–220.
6. Shikinami, Y., & Okuno, M. (1999). Bioresorbable device made of forged composites of hydroxyapatite (HA) particles and poly-L-Lactide (PLLA): Part I: Basic characteristics. *Biomaterials, 20*, 859–877.
7. Fu, X. M., Oshima, H., Araki, Y., Narita, Y., Mutsuga, M., Okada, N., et al. (2013). A comparative study of two types of sternal pins used for sternal closure: poly-L-lactide sternal pins versus uncalcined hydroxyapatite poly-L-lactide sternal pins. *Journal of Artificial Organs, 16*, 458–463.
8. Nikolaou, V. S., Korres, D., Xypnitos, F., Lazarettos, J., Lallos, S., Sapkas, G., & Efstathopoulos, N. (2009). Fixation of Mitchell's osteotomy with bioabsorbable pins for treatment of hallux valgus deformity. *International Orthopaedics, 33*, 701–706.
9. Walsh, S. J., Boyle, M. J., & Morganti, V. (2008). Large osteochondral fractures of the lateral femoral condyle in the adolescent: Outcome of bioabsorbable pin fixation. *Journal of Bone and Joint Surgery, American Volume, 90*, 1473–1478.
10. Min, W., Munro, M., & Sanders, R. (2010). Stabilization of displaced articular fragments in calcaneal fractures using bioabsorbable pin fixation: A technique guide. *Journal of Orthopaedic Trauma, 24*, 770–774.
11. Cheung, J. T. M., An, K. N., & Zhang, M. (2006). Consequences of partial and total plantar fascia release: A finite element study. *Foot and Ankle International, 27*, 125–132.
12. Lee, J. Y., & Lee, Y. S. (2011). Optimal double screw configuration for subtalar arthrodesis: a finite element analysis. *Knee Surgery, Sports Traumatology, Arthroscopy, 19*, 842–849.
13. Liang, J., Yang, Y., Yu, G., Niu, W., & Wang, Y. (2011). Deformation and stress distribution of the human foot after plantar ligament release: a cadaveric study and finite element analysis. *Science China Life Science, 54*, 267–271.
14. Lin, Y. H., Chen, A. C. Y., Kou, H. N., Yu, T. C., Sun, M. T., & Lin, C. L. (2013). Biomechancial evaluation of modified dorsal double-plating fixation with adjustable joint and microthread designs for comminuted extra-articular distal radius fractures. *Journal of Medical and Biological Engineering, 33*, 29–34.
15. Xu, H., Tang, H., Guan, X., Jiang, F., Xu, N., Ju, W., et al. (2013). Biomechanical comparison of posterior lumbar interbody fusion and transforaminal lumbar interbody fusion by finite element analysis. *Neurosururgery, 72*, 21–26.
16. Sutawan, B., Atitsa, P., & Kongkiat, K. (2008). Synthesis and mechanical properties of poly (LLA-co-DLLA) copolymers. *Journal of Metals Materials and Minerals, 18*, 175–180.

17. Niu, W., & Ding, Z. (2007). Comparative study on three different methods applied to establish 3D finite element calcaneus model. *Journal of Medical Biomechanics, 22*, 345–350.
18. Hurschler, C., Emmerich, J., & Wülker, N. (2003). In vitro simulation of stance phase gait part I: Model verification. *Foot and Ankle International, 24*, 614–622.
19. Niu, W., Chu, Z., Yao, J., Zhang, M., Fan, Y., & Zhao, Q. (2012). Effects of laterality, ankle inversion and stabilizers on the plantar pressure distribution during unipedal standing. *Journal of Mechanics in Medicine and Biology, 12*, 1250055.
20. Niu, W. X., Yao, J., Chu, Z. W., Jiang, C. H., Zhang M., & Fan, Y. B. (2015). Effects of ankle eversion, limb laterality, and ankle stabilizers on transient postural stability during unipedal standing. *Journal of Medical and Biological Engineering, 35*, 69–75.
21. Zhang, J., Ebraheim, N., Lausé, G. E., Xiao, B., & Xu, R. (2012). A comparison of absorbable screws and metallic plates in treating calcaneal fractures: a prospective randomized trial. *Journal of Trauma Acute Care Surgery, 72*, 106–110.
22. Zhang, J., Xiao, B., & Wu, Z. (2011). Surgical treatment of calcaneal fractures with bioabsorbable screws. *International Orthopaedics, 35*, 529–533.
23. Wang, C. L., Chang, G. L., Tseng, W. C., Yu, C. Y., & Lin, R. M. (1998). Strength of internal fixation for calcaneal fractures. *Clinical Biomechanics, 13*, 230–233.
24. Redfern, D. J., Oliverira, M. L. R., Campbell, J. T., & Belkoff, S. M. (2006). A biomechanical comparison of locking and non-locking plates for the fixation of calcaneal fracture. *Foot and Ankle International, 27*, 196–201.
25. Nelson, J. D., McIff, T. E., Moodie, P. G., Iverson, J. L., & Horton, G. A. (2010). Biomechanical stability of intramedullary technique for fixation of joint depressed calcaneus fracture. *Foot and Ankle International, 31*, 229–235.
26. Richter, M., Droste, P., Goesling, T., Zech, S., & Krettek, C. (2006). Polyaxially-locked plate screws increase stability of fracture fixation in an experimental model of calcaneal fracture. *Journal of Bone and Joint Surgery, 88*, 1257–1263.
27. Wang, C. L., Cheng, C. K., Chen, C. W., Lu, C. M., Hang, Y. S., & Liu, T. K. (1995). Contact area and pressure distribution in the subtalar joint. *Journal of Biomechanics, 28*, 269–279.
28. Giddings, V. L., Beaupré, G. S., Whalen, R. T., & Carter, D. R. (2000). Calcaneal loading during walking and running. *Medicine and Science in Sports and Exercise, 32*, 627–634.
29. Wagner, U. A., Sangeorzan, B. J., Harrington, R. M., & Tencer, A. F. (1992). Contact characteristics of the subtalar joint: load distribution between the anterior and posterior facets. *Journal of Orthopaedic Research, 10*, 535–543.